Investigation of shock control bump geometry variation on oblique shock wave boundary layer interactions

Bulut, J.; Schrijer, F.F.J.; van Oudheusden, B.W.

Publication date
2023

Document Version
Final published version

Published in
57th 3AF International Conference

3AF Association Aéronautique et Astronautique de France

57th 3AF International Conference on Applied Aerodynamics
29 — 31 March 2023, Bordeaux – France

AERO2023-68-BULUT

INVESTIGATION OF SHOCK CONTROL BUMP GEOMETRY VARIATION ON OBLIQUE SHOCK WAVE BOUNDARY LAYER INTERACTIONS

J. Bulut[(1)] , F.F.J. Schrijer[(2)] and B.W. van Oudheusden[(3)]

[(1)]TU Delft Faculty of Aerospace Engineering, Kluyverweg 1, 2629HS Delft, The Netherlands, J.Bulut@tudelft.nl

[(2)]TU Delft Faculty of Aerospace Engineering, Kluyverweg 1, 2629HS Delft, The Netherlands, F.F.J.Schrijer@tudelft.nl

[(3)]TU Delft Faculty of Aerospace Engineering, Kluyverweg 1, 2629HS Delft, The Netherlands, B.W.vanOudheusden@tudelft.nl

ABSTRACT

The interaction between a shock wave and a boundary layer is a topic of primary relevance in high-speed aerodynamics, as it may deteriorate the vehicle performance, and can even lead to structural damage. Over the years, many researchers have investigated various control techniques to mitigate the detrimental effects of such shock wave boundary layer interactions (SWBLI). In this experimental study the effect of shock control bumps (SCB) on oblique shock wave/boundary layer interactions is investigated, notably the influence of the ramp section of the bump. To study the effect, varying bump geometries were designed with 5 different ramp angles while the maximum crest height is kept constant. The experiments were conducted in the ST-15 wind-tunnel at the Delft University of Technology for fully developed turbulent boundary layer conditions with Re_θ of 21.8 10^3 and freestream Mach number of 2.0. The effectiveness is assessed from the size of the separated flow region, as well as the downstream boundary layer velocity profile. For this, PIV is employed as the main diagnostic method to characterise the flow field. In addition to this, high-speed Schlieren and oil flow measurements were performed to asses the effect of the SCB on the overall interaction structure.

1. INTRODUCTION

The occurrence of shock waves is a prominent feature of high speed flight. There are many potential consequences of the shock wave formation for the vehicle performance. For instance, the adverse pressure gradient caused by the shock impingement on the boundary layer can result in a partly flow reversal in the boundary layer flow. Such separation bubbles typically cause a drastic increase in drag while leading to high total pressure losses. Moreover, they introduce high levels of unsteadiness in the flow.

Over the years, developing control methods to mitigate the undesired effects of shock wave boundary layer interactions has been in the focus of many researchers. Most of these methods aim to act on the low momentum region of the boundary layer. Some, such as boundary layer bleed, aim to mitigate the negative effects by removing the low momentum portion of the boundary layer, thus making it fuller in shape, and hence more resistant to separation. Other target to energize the boundary layer by increased mixing. This can be achieved by introducing counter rotating vortices, hence, such devices are referred as vortex generators. Especially, sub-boundary layer vortex generators have been widely investigated over the years due to their efficiency in promoting the momentum of the boundary layer without introducing strong adverse effects on drag.

An alternative method to alleviate the unfavourable effects of the shock wave boundary layer interactions is by controlling the shock formation.Due to their geometry, shock control bumps (SCB) have been used for reducing the wave drag of especially transonic wings by means of modifying the shock structure. The bump geometry generates quasi-isentropic compression waves upstream of the normal shock wave resulting in a λ-shock configuration. The flow passing through these isentropic compression waves gradually decreases its velocity; thus, the bump partly eliminates the abrupt effects caused by a single, strong normal shock wave.

Various studies have assessed the effectiveness of the shock control bumps for normal shock wave boundary layer interactions control. In [7] Ogawa et al. investigated different 3D bump geometries in a M=1.3 flow. They observed the dependence of the shock structure in relation to the impingement location on the bump surface. It was found that when the shock impinges on the upstream part of the bump, re-accelerated flow can create a “supersonic tongue” downstream which induces undesired secondary shock structures and an increase in the wave drag might occur [7]. In contrast, a downstream impinging shock can cause a secondary λ-shock structure formation due to the expansion of the flow passing over the crest of the bump.

Whereas most studies on the effects of SCBs have been for normal shock wave boundary layer interactions, relatively limited research has focused on the flow structures generated by the combination of oblique SWBLIs and shock control bumps. Considering the shape of the SCB, its effect is expected to downsize the separation by ”filling” the separation bubble with the bump structure. This may be expected also to restrict the dynamics of the flow separation region, thereby reducing the overall interaction unsteadiness. In addition, the streamwise vortices introduced to the downstream of the interaction by the 3D SCB, would promote a faster recovery of the boundary layer flow. Moreover, the gradual flow expansion caused by the tail portion of the bump also contributes to a faster flow recovery and providing a fuller velocity profile in respect to the uncontrolled case.

The focus of interest and objective of this work is to improve the understanding of the flow physics associated to the application of 3D SCB in oblique shock wave turbulent boundary layer interactions. In a previous study [2], the effect of the shock impingement location was studied, while this follow-up investigation considers the effect of the bump geometry. In light of the information gained from the research on the interaction between a SCB and a normal shock waves [7], a set of experiments have designed in TU Delft to investigate the effect of the impingement location of the incident shock on the bump surface. In this work, three different shock impingement locations were selected as following: the reference control impingement location corresponding to the 1.5δ upstream of the first point where the bump has the maximum height,as well as 1.5δ downstream and 1δ upstream of the control location. The assessment of the effectiveness of SCB is done through effectiveness on reducing the reversed flow caused by the shock impingement. This investigation revealed that the control impingement case delivers approximately 70% improvement of the probability of local flow reversal, P_{sep}, compared to the uncontrolled case. Therefore, in the current study the incident shock impingement location is set approximately at 1δ upstream of the first point where the bump reaches its maximum height. The current study investigates the effect of different SCB geometries in terms of the change in the angle of the ramp section of the bump.

The topic of the current study is the experimental assessment of the impact of the bump geometry on the interaction, in terms of both the the mean flow field characteristics and its level of unsteadiness. The unsteady dynamics of the SWBLI are aimed to be investigated by means of high speed Schlieren measurements. However, the results remained to be inconclusive due to the act that highly 3D flow is not well representative by the Schlieren results. Quantitative information on the flow field is obtained from PIV measurements. With this data, a further quantification of the velocity gradients and interaction structure is carried out for the cases with and without SCB.

2. EXPERIMENTAL ARRANGEMENT

2.1 Flow facility and experimental investigation

This transition is very abrupt. Make a smoother transfer between the (suggested) working principle to the objective of the study. of the SWBLI are aimed to be investigated by means of high speed Schlieren measurements. However, the results inconclusive due to the fact that with the SCB introduced the SWBLI becomes even more 3D and as a result the flow is not well characterised by the Schlieren results. Quantitative information on the 3D flow field is obtained from PIV measurements. With this data, a further quantification of the velocity gradients and interaction structure is carried out for the cases with and without SCB.

The experiments were carried out in the ST-15 blowdown supersonic wind-tunnel of the Delft University of Technology. The test section of the tunnel has dimensions of 150 mm x 150 mm and has glass windows in the side walls which allow optical access. In the experiments, the tunnel is operated at a Mach number of 2.0, a total pressure p_0 of 3.0 bars and a total temperature T_0 of approximately 290 K. In [5] Giepman et al investigated the effects of location and size of micro-ramp vortex generators in the same facility at similar operating conditions and have also documented the undisturbed boundary layer. A summary of the main flow conditions is given in the Table 11.

The bottom wall of the tunnel, where the boundary layer thickness is approximately δ_{99}=5.2 mm [5], is used to assess the uncontrolled SWBLI flow field. Subsequently, a shock control bump is installed on this wall by using double sided adhesive tape. For all the cases, the incident shock is generated by installing a 12ĉirc shock generator.

Table 1: Experimental conditions and undisturbed boundary layer properties [5]

Parameter	Value	Parameter	Value
M_∞	2.0	δ_i	0.63
U_∞ [m/s]	520	θ_i	0.52
P_0 [N/m^2]	3 x 10^5	H_i	1.23
T_0 [K]	290	Re	42 x 10^6
δ_{99} [mm]	5.2	Re_θ	21.8 x 10^3

2.2 Shock control bump specifications

Introducing a SCB geometry in the interaction region directly modifies the interaction structure (see Fig. 2). A typical SCB consists of a ramp, a short crest and a tail part. As mentioned before, in a highly supersonic flow the initial, ramp, part of the bump acts as a compression ramp that introduces a secondary shock into the interaction. This secondary shock, which originates at the leading edge of the bump, decelerates the flow upstream of the impinging shock. This could alleviate the detrimental effects of a strong impinging-separation shock system and possibly even removing any separated region from the flow.

In case the bump geometry has a high ramp angle it would cause a strong compression corner interaction at the leading edge of the bump and this might induce an undesired separation of the flow. Therefore, it is important to know the maximum shock intensity that the incoming flow boundary layer could withstand without separating. The state of the flow separation highly depends on the shock strength, in other words the upstream Mach number of the flow and the pressure rise caused by the shock wave. According to Ginoux [6] the formation of separation is independent of the Reynolds number for high Reynolds number flows. Souverein et al. [9] established a global model for a separation state criterion, from analyzing the collected data from compression corner and incident-reflection shock interactions investigated by different research groups at different flow conditions. They observed a Reynolds number dependency, which was modelled with a coefficient that slightly differs in value between the high and low Reynolds flows. A widely accepted criterion is derived from the free-interaction theory [1] 1. In this criterion the Reynolds number effect is also taken into account through the friction coefficient of the undisturbed boundary layer, C_{f_o}.

$$\Delta p_{sep} = k\gamma M_0^2 \sqrt{\frac{2C_{f_o}}{(M_0^2-1)^{1/2}}} \tag{1}$$

For $Re_\theta \leq 10^4$ the coefficient k would be 3.0 and for $Re_\theta < 10^4$ k would be 2.5. Through this coefficient and the C_{f_0}, the effect of the Reynolds number is taken into account in the estimation of the separation criterion. Knowing the upstream Mach number, M_0, and the friction coefficient, for the present conditions the separation would be expected when there would be a minimum pressure jump of Δp_{sep} of 1.79. Accordingly, the maximum SCB ramp angle, θ_{ramp}, which the boundary layer can withstand without separating would be approximately 14.0°. Therefore, for the bump designs chosen in this study, a flow separation caused by the compression shock wave originated from the leading edge of the SCB is not expected to occur.

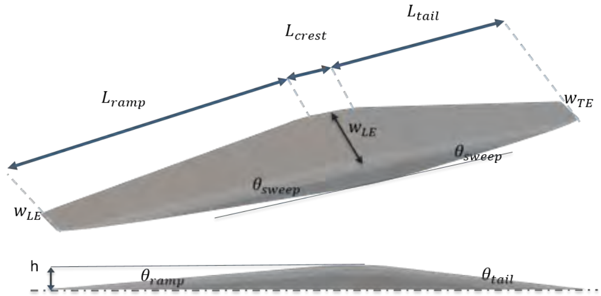

Figure 1: SCB geometry.

Additionally, the SCB ramp angle for the baseline geometry is chosen to minimize the undesired effects of the shock wave in the flow. It is expected to have a total pressure loss when a shock forms in a supersonic flow. Therefore, it is crucial to optimize the modified shock system for minimizing the total pressure loss. In this work, a well-known method that has been used to optimize the total pressure loss in a supersonic engine inlet is applied to the baseline SCB geometry design. Oswatitsch [8], suggested that the maximum pressure recovery in a supersonic inlet is obtained when the subsequent shocks are equal of strength. Crossing a shock creates a sudden increase in the temperature. In case the two subsequent shocks do not result in the same entropy increase, the weaker one will be outweighted by the strong entropy increase [3]. By having the equal normal Mach number upstream of the each subsequent oblique shock one can optimize the multiple shock shock system for the total pressure recovery. In the case of placing the SCB such that the leading edge of the bump will be at the upstream of a conventional incident-reflected shock structure, a similar subsequent shock system can be obtained. Interpreting the SCB leading edge shock and the separation shock of the SWBLI as similar set of oblique shocks as occurs in a spersonic inlet, ensuring the minimization of the total pressure loss would be achieved by a SCB geometry where the resulting leading edge shock and the following separation shock would have same strength. In other words, by introducing the bump geometry in the flow, separation shock is aimed to be broken down into two oblique shock waves with equal strength. The flow deflection caused by the separation shock is obtained from the PIV measurements of the uncontrolled interaction and therefore, for the known upstream flow conditions the separation shock strength is acquired. Once the flow deflection and the overall pressure jump caused by the separation shock is obtained, the optimum flow deflection angle due to the ramp portion of the bump is set as 4.6 °. Therefore, a baseline geometry is designed such that the leading edge shock would be in the same strength of the separation shock wave in the modified interaction structure. The dimensions for the different SCB geometries are shown in Table (2). Overall 5 different bump geometries are tested where the tail portion of the bump and the height of t he crest is kept constant and the ramp angle, θ_{ramp}, is set in different values around baseline angle.

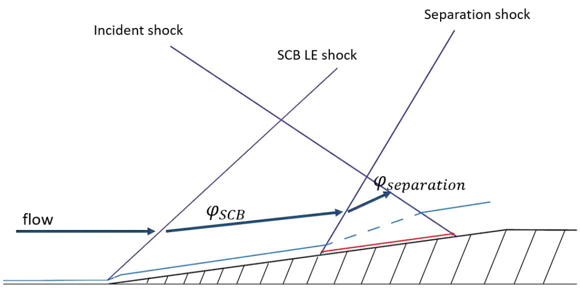

Figure 2: Schematic representation of the interaction structure with the bump geometry.

Table 2: Geometrical parameters of SCBs.

Configuration	height [mm]	θ_{ramp}	θ_{tail}
r4_h5	5	4°	6.25°
4p6_h5	5	4.6°	6.25°
r5p4_h5	5	5.4°	6.25°
r6p25_h5	5	6.25°	6.25°
r7p25_h5	5	7.25°	6.25°

2.3 Experimental setup

Two main flow diagnostic methods are used in this study, high-speed Schlieren visualization and PIV. Additional information on the interaction structure is obtained from surface oil flow visualization.

High-speed Schlieren is used to resolve the unsteady dynamics of the SWBLI. A LaVision ProHS camera is used with an acquisition frequency of 6250 Hz which is sufficient to resolve the major separation shock unsteadiness.

To capture the interaction region where the incident shock impinges on the bump surface and the downstream flow, planar PIV measurements were performed with two

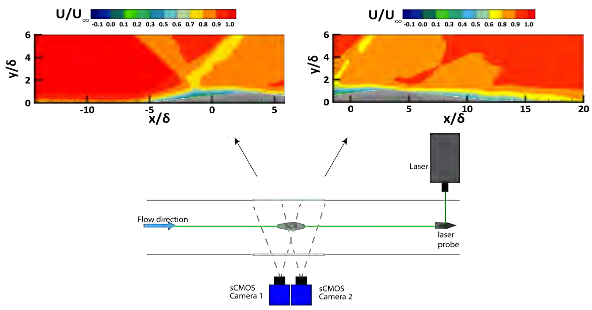

Figure 3: Setup of experiments.

partially overlaping fields of view. The set-up for the 2D2C PIV is shown schematically in Fig. 3, indicating two the LaVision sCMOS cameras with 5.5 MP. One of the cameras was zoomed in on the interaction region while the other was focused on the downstream region of the interaction. An overlap of approximately 6 mm was provided to allow proper combination of the datasets (see Fig. 3) The full width and the height of the combined FOV is 32.2δ (167.4 mm) and 6.5δ (33.8 mm). On both cameras a 105 mm Nikkor objective was used with f# set to 8. For the illumination, a Quantel Evergreen double-pulsed Nd:YAG laser is used, operating at a pulse energy of 200 mJ/pulse with a repetition rate of 15 Hz. For all the measurements the pulse separation is set to 1 μs. Measurements were carried out in the symmetry plane of the bump.

Data acquisition and processing is done in DaVis 8.4.0. As the first step a Butterworth high pass filter is applied to filter the reflections. Additionally, for the pre-processing the particle intensity was normalized using min/max filtering. Next, a multi pass cross-correlation with 64 pixels and 24 pixels respectively, with 75% overlap were applied. This resulted in a vector pitch of 0.3 mm or approximately 0.06δ. As final step, the universal outlier detection approach was applied, as implemented in DaVis. Average velocity field and standard deviation of the vector field are also obtained through DaVis. To do so, a requirement of having at least 50 source vectors at each position to compute results is implemented.

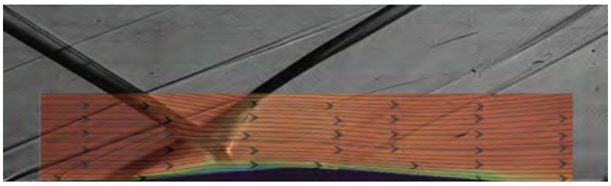

Figure 4: Average flow field for $\theta_{ramp} = 5.4°$ of overlapping FOV for Schlieren and FOV of PIV from two cameras.

3. RESULTS

3.1 Interaction visualization

In the Fig. 2 the interaction between incident-reflection shock wave structure and the boundary layer is represented schematically for the controlled interaction. Where in the uncontrolled, natural, the interaction impingement of a strong incident shock causes an adverse pressure gradient on the boundary layer and results in separation of it. The separation shock forces a deflection of the flow caused by the thickening of the boundary layer. The SCB changes this interaction structure as shown in the Fig. 2. The leading edge shock slows down the flow upstream of the separation shock. As described in section 2.2, the separation state of the flow is dependent on the shock strength where it is defined by the flow deflection and upcoming mach number of the flow. One can say the bump structure can be used to act on the shock strength to remove the flow separation.

In Fig. 5 images obtained from Schlieren visualization show the global features of the uncontrolled and controlled interactions. The incident shock is generated by a 12ĉirc shock generator and the reflected shock is formed approximately 6δ_{99} upstream of the impinging location of the incident shock on the wall for the uncontrolled interaction. Downstream of the interaction, it can be seen that the boundary layer is growing in thickness. The shock impingement location is kept unchanged over the experiments where it coincides to 1δ upstream of the crest edge for all SCB geometries. Schlieren is a visualization technique which integrates the density gradient over the full span of the test section. The width of the SCB is 4δ where the test section width is 30δ. From the oil flow visualizations for the uncontrolled interaction (see Fig. 6) the extend of the corner interactions obtained as around 4δ each side. When the flow structures seen in the schlieren images analysed with the oil flow visualizations, the formation of the leading edge shock is confirmed with the cases with the SCB. In addition to that, an expansion fan over the bump crest can also be observed as expected.

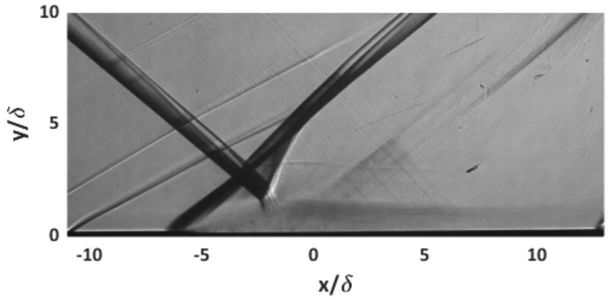

(a) *Uncontrolled case.*

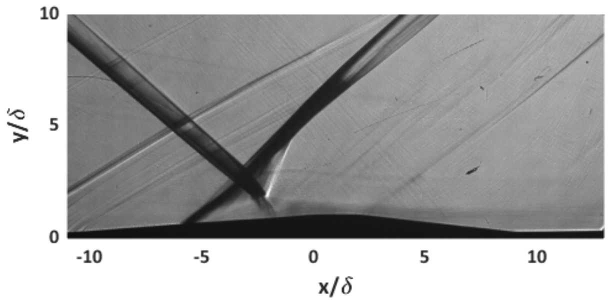

(b) *SCB with* $\theta_{ramp} = 4°$

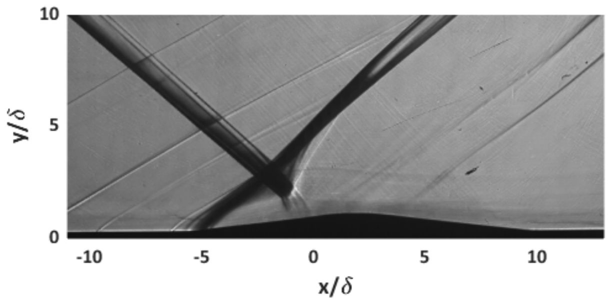

(c) *SCB with* $\theta_{ramp} = 7.25°$

Figure 5: Average flow field obtained from Schlieren measurements.

In Fig. 6 surface flow topology can be seen from the obtained oil flow images. The separation and reattachment lines are indicated for all the cases. All images were taken after the wind tunnel runs were completed. Therefore the footprint of the separation shock exhibits not a quasi one dimensional line, especially for the cases where the oil had accumulated. The oil flow visualization for the uncontrolled case results in relatively 2D separation and reattachment lines, however the corner effects and the strong interaction is not allowing to have a fully 2D interaction over the span. Moreover, the cases with the SCB are showing strong evidence on the highly 3D interaction induced by the 3D shape of the bump geometry. The darker regions downstream of the bump in all cases may suggest the vortex production in the wake of the SCB. Colliss et al. [4] suggested that these vortices originate from the ramp of the bump. This indicates that these vortices might originate from the focal points forming over the bump. While it is relatively easy to identify the separation and reattachment lines on the uncontrolled portions of the test section for the controlled cases, identifying the flow structures over the bump from the oil flow visualizations is more challenging. Nonetheless,the obtained flow topology from the oil flow visualizations indicates strong evidence of the 3D flow structure for the interaction between SCB and SWBLI. This strong non-uniformity on the spanwise direction makes getting spectral information on the shock oscillations from the schlieren images

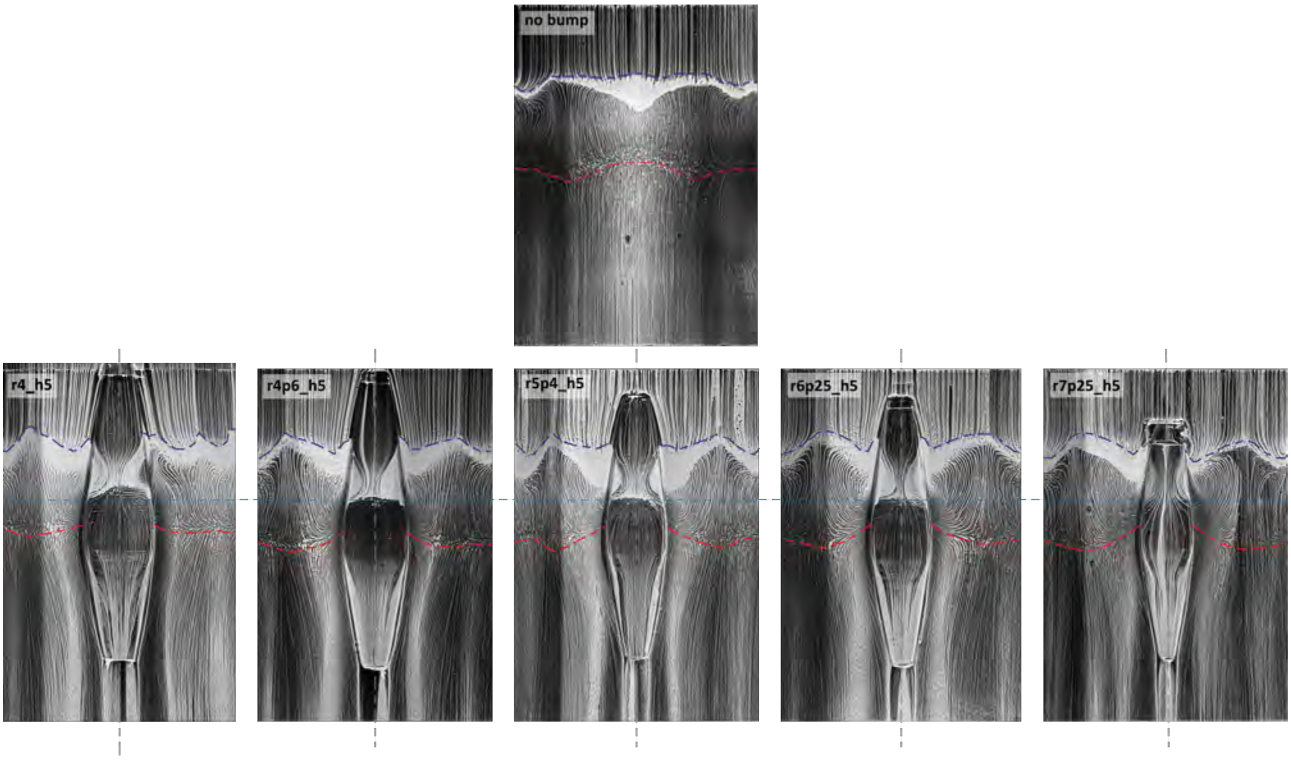

Figure 6: Oil flow visualizations of the all SCB cases and the uncontrolled case (Dark blue line shows the separation and red line shows the reattachment line. Light blue dashed line indicates the unviscid impinging location of the incident shock on the bump surface).

more complicated .

3.2 Flow field characterization

The average flow fields obtained from PIV for horizontal and vertical velocity components are given in Fig. 7 and Fig. 8, respectively. Streamlines obtained from the velocity gradients are plotted over the mean vertical velocity contour for controlled and uncontrolled cases (see Fig. 8). This confirms that the flow deflection caused by the incident shock is 12°. Nonetheless, the flow deflection obtained from the flow after the separation shock foot is approximately 9°. An inviscid flow analysis for the shock reflection at a freestream Mach number of 2.0 and an incident shock formed by a 12° shock generator, predicts a weak shock solution for a strong interaction with pressure rise across the incident shock P_i/P_0 as 1.89, and the pressure rise over the entire interaction to be approximately P_1/P_0 =3.48. On the other hand, when the measured flow deflection is taken into account in this estimation the value of pressure increase would be approximately P_1/P_0 =3.0.

The interaction structure shows differences depending on the parameters. One could say optimization between the distance between these two interactions plays an important role in the interaction structure hence the effectiveness of the bump. The shock impingement location should be sufficiently away from the corner interaction such that giving enough time to the boundary layer to recover. Therefore, the inviscid shock impingement location is set approximately 1 δ upstream of the start of the bump crest. Additionally, change in the ramp angle modifies the distance between corner and shock incident shock interactions where the maximum height of the bump is set approximately as the upstream boundary layer thickness (5.2 mm).

To understand the effect of this distance on the change of the interaction structure we can look in the two extreme cases, $\theta_{ramp} = 4°$ and $\theta_{ramp} = 7.25°$ (see 8). The oil flow visualizations have shown strong evidences for the 3D flow for the controlled cases, however with the assumption of having a 2D flow on the PIV measurement plane one could have estimation for the pressure change through the interaction. When flow deflections in the interaction region obtained from PIV measurements are taken into account to estimate the pressure gradient through the interaction by the isentropic relations for case of the bump with the $\theta_{ramp} = 7.25°$ degrees, overall pressure jump across the interaction region is found approximately $\Delta_p = 2.5$. The same procedure is followed for the case of the bump with the $\theta_{ramp} = 4.6°$ and it resulted in a pressure jump estimation of approximately $\Delta_p = 3$.

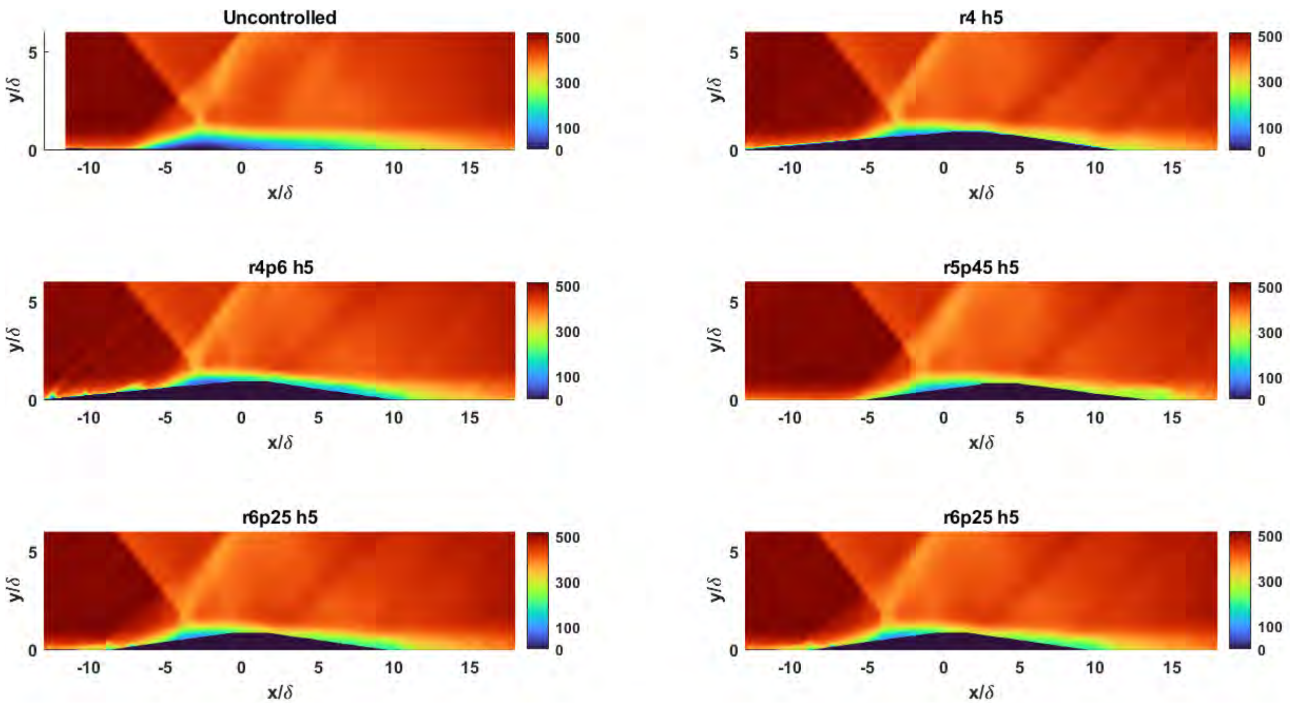

Figure 7: Mean streamwise velocity contour for all cases.

Fig. 7 compares the flow topology for cases with three different bump geometry configurations and case without a bump. Where for the natural interaction case flow separation can be observed over the mean flow field, no average separation takes place for the cases with the SCB. Albeit having no reversed flow in the mean flow field, local flow separation can be observed in the instantaneous snapshots of the flow with SCB.

In Fig. 9, turbulent intensity in the interaction region is plotted. Which indicates the level of velocity fluctuations over the mean velocity. In all the cases, the velocity fluctuations shows increase throughout the interaction region. The larger velocity fluctuations can be associated to the development of vortical structures. Fig. 9 shows the the higher turbulent intensity levels have been recorded for the uncontrolled case over the shear layer. This could be interpreted as the higher production of the vorticity due to the boundary layer separation. Placement of the SCB has reduced the turbulent intensity for the case with all SCB geometries. Additionally, the uncontrolled case presents higher turbulence levels over a larger extend in the streamwise direction compared to the cases with the SCB. On contrary, in the cases with the SCB lower turbulence levels are encountered downstream of the interaction. Lower velocity fluctuations could be interpreted as having a more stable velocity profile.

4. CONCLUSIONS

An experimental investigation was performed to improve the understanding of the interaction between SCB and SWBLI on the flow. The freestream flow conditions correspond to a Mach number of 2.0, a unit Reynolds number Re of 42 10^{6}, and a momentum thickness Reynolds number Re_{θ} of 21.8 10^{3}, while the shock generator's flow deflection angle is set to 12°.

High-speed Schlieren measurements are used to investigate the effect of the SCB on the SWBLI flow dynamics. Measurements are performed for five different ramp angles of SCB compared to the uncontrolled case. However, due to the limitations introduced by by the spanwise integration effect of Schlieren technique no conclusion on the unsteady characteristics couldn be drawn. In all cases, SCB was covering approximately one sixth of the test section on spanwise direction. Therefore, the interaction is not controlled over a significant extent of the test section and the visualization of the controlled interaction is contaminated by the large region where it is not controlled. To overcome this limitation an investigation with a 2D SCB design is planned.

PIV measurements were performed to visualize the flow organization in an uncontrolled oblique shock turbulent boundary layer interaction and the case of this interaction controlled by SCB. The investigation was carried out for all different bump geometries. This investigation revealed the distance between the weak compression shock originated from the leading edge of the bump

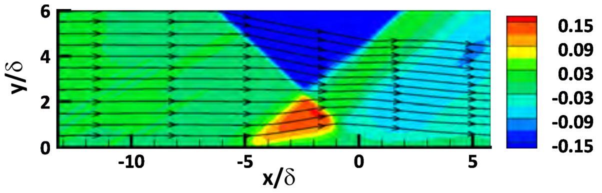

(a) *Uncontrolled case.*

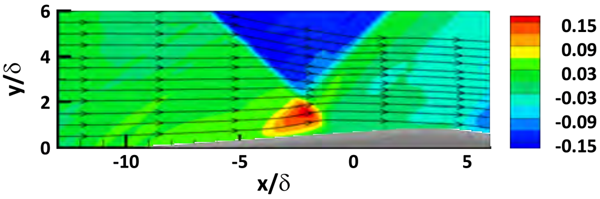

(b) *SCB with* $\theta_{ramp} = 4°$.

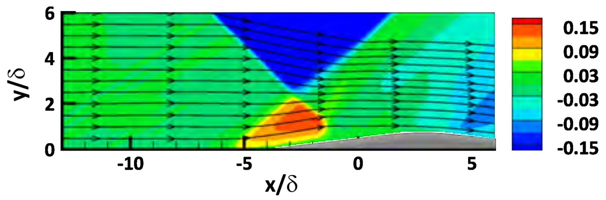

(c) *SCB with* $\theta_{ramp} = 7.25°$.

Figure 8: Streamlines over the vertical velocity contour in the interaction region.

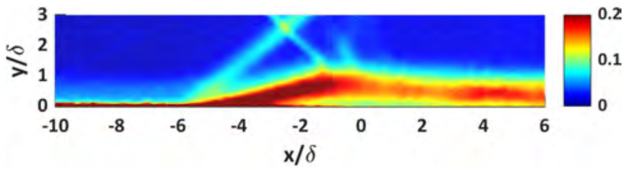

(a) *Uncontrolled case.*

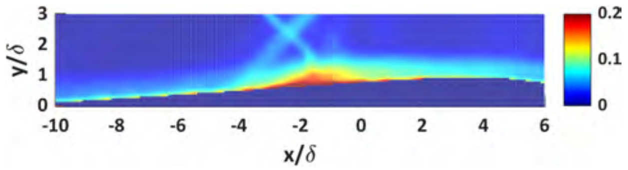

(b) *SCB with* $\theta_{ramp} = 4°$.

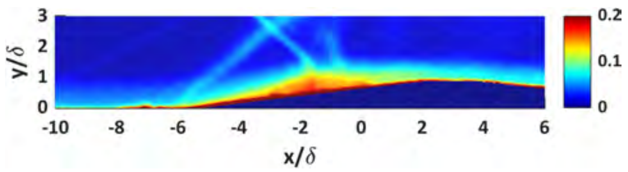

(c) *SCB with* $\theta_{ramp} = 7.25°$.

Figure 9: Turbulent intensity in the interaction region.

and the main interaction plays a crucial role to optimize the SCB performance. Where the height of the bump is kept constant, cases with the lower ramp angles resulted in lower interaction length values.

The turbulent intensity over the interaction region was determined for all cases, including the uncontrolled case. Overall turbulent intensity decreased significantly for the controlled cases. Lower ramp angle geometries delivered lower turbulent intensity levels alongside the reduction on the interaction length. Moreover, in comparison with the uncontrolled case turbulent intensity levels are observed significantly lower at the downstream of the interaction for the all cases with the bump.

To improve the performance of the SCB in reducing the separation of the flow a further design modification on the bump geometry, in which the bump better "fills" the separation bubble, is proposed. In addition to this, it would be important to characterize the effect of installing a SCB in the interaction region on the overall drag to have the better assessment of the efficiency of the SCB as a control device.

REFERENCES

[1] H. Babinsky and J. Harvey. *Shock Wave-Boundary-Layer Interactions*. Cambridge Aerospace Series, Ed. 2011.

[2] J. Bulut, F.F.J. Schrijer, and B.W. van Oudheusden. Effect of shock control bumps on oblique shock wave turbulent boundary layer interactions. In *56th 3AF International Conference on Applied Aerodynamics*, 2022.

[3] T. Cain. Design and evaluation of high speed intakes. *NATO*, 2011.

[4] S. P. Colliss, H. Babinsky, K. Nübler, and T. Lutz. Vortical structures on three-dimensional shock control bumps. *AIAA Journal*, 54 (8), 2016.

[5] R. Giepman, F.F.J. Schrijer, and B.W. van Oudheusden. Flow control of an oblique shock wave reflection with micro-ramp vortex generators:effects of location and size. *Physics of Fluids*, 26 (6), 2014.

[6] J.J. Ginoux. Interaction entre ondes de choc et couches limites. *Chocs et Ondes de Choc,*, 2 (8), 1970.

[7] H. Ogawa, H. Babinsky, M. Pätzold, and T. Lutz. Shockwave/boundary-layer interaction control using three-dimensional bumps for transonic wings. *AIAA Journal*, 46 (6):1442–1452, 2008.

[8] K. Oswatitsch. The pressure recovery on jet-propelled projectiles at high supersonic speeds. *Forschungen und Entwicklungen des Heereswaffenamtes (Research and Development of the Army Weapons Office)*, No. 1005, 1944.

[9] L. G. Souverein, P. G. Bakker, and P. Dupont. A scaling analysis for turbulent shock-wave/boundary-layer interactions. *Journal of Fluid Mechanics*, vol. 714:505–535, 2013.